J Electr Eng Technol.2017; 12(5): 2043-2050
http://doi.org/10.5370/JEET.2017.12.5.2043

ISSN(Print) 1975-0102
ISSN(Online) 2093-7423

# Capacity Firming for Wind Generation using One-Step Model Predictive Control and Battery Energy Storage System

**Micro Daryl Robles*, Jung-Su Kim† and Hwachang Song***

**Abstract** – This paper presents two MPC (Model Predictive Control) based charging and discharging algorithms of BESS (Battery Energy Storage System) for capacity firming of wind generation. To deal with the intermittency of the output of wind generation, a single BESS is employed. The proposed algorithms not only make the output of combined systems of wind generation and BESS track the pre-defined reference, but also keep the SoC (State of Charge) of BESS within its physical limitation. Since the proposed algorithms are both presented in simple if-then statements which are the optimal solutions of related optimization problems, they are both easy to implement in a real-time system. Finally, simulations of the two strategies are done using a realistic wind farm library and a BESS model. The results on both simulations show that the proposed algorithms effectively achieve capacity firming while fulfilling all physical constraints.

**Keywords**: Wind generation, MPC (Model Predictive Control), Capacity firming, SoC (State of Charge), BESS (Battery Energy Storage System)

## 1. Introduction

The increased demand towards renewable energy as a sustainable power resource is hampered by stability and reliability issues when it is integrated to the grid. While the technology of harnessing the power of both wind and solar has improved over the recent years, creating a huge farm based on them and establishing them as the base power pose huge stability issues. This is primarily because of the intermittent nature of renewable energy [1-3], which results in power output with sudden ups and downs. Due to this nature, a large wind farm usually needs a huge energy storage system and a good control algorithm to firm its output and make it more suitable for the grid. Designing a good controller for the operation of the wind farm with energy storage can largely improve its stability and thus maximize the contribution of wind energy to the grid.

The focus of this research is about the smoothing of the power output of wind farm using energy storage systems. This is also called capacity firming, which makes the output of combined systems of wind generation and BESS track the pre-defined reference so that it can be dispatched properly to the grid for a given time period. There are several control algorithms in the literature that implement renewable capacity firming, and some of these focus on output smoothing only and not firming, in the sense that it only removes the jitter, but does not really maintain the output to a constant level [4]. Other approaches have tried to combine Capacity Firming with other energy storage applications such as Energy Time Shifting [5]. However, it poses some conflict between the two applications, depending on what is the priority application during that time of the day. As for capacity firming, there are research results that depend on specifying a reference level to maintain the output of the wind farm, and this reference level is either based on the forecasting of the wind power [6-9] or the forecasting of the energy price on the market [10]. Most of these methods do not consider the constraints of the Battery Energy Storage System (BESS) into their solution explicitly, and thus check the SoC in an ad-hoc manner to confirm if it is still within the bounds of the constraints to avoid instability.

In this paper, a one-step ahead model predictive control (one-step MPC) is proposed. The MPC is a repeated application of finite horizon optimal control. The motivation of employing the MPC as the controller is based on its inherent capability of anticipating the dynamic behavior of the system in the near future and handling the physical constraints of the BESS. Note that existing results (for example, PID control) do not consider the SoC constraints systematically. Furthermore, MPC considers the performance of the system by optimizing a cost function that describes the objective of the controller, which in this case is capacity firming. Lastly, since an MPC computes for an optimal solution repeatedly over the whole time period, a one-step horizon was practically chosen for faster computation which is very applicable for a real-time environment.

The contribution of this paper is twofold. First, two MPC-based charging and discharging strategies are proposed, which make the output of the system follow the given reference while fulfilling the physical constraints on the

† Corresponding Author: Dept. of Electrical and Information Engineering, SeoulTech, Korea. (jungsu@seoultech.ac.kr)
* Dept. of Electrical and Information Engineering, SeoulTech, Korea. (microdaryl@gmail.com, hcsong@seoultech.ac.kr)
Received: December 30, 2016; Accepted: May 1, 2017

BESS. Moreover, using the analytic solution of an MPC with one-step prediction horizon, the proposed MPC-based algorithm is presented as a look-up table, which makes it possible for the proposed algorithm to be implemented in practice as well. Second, a realistic simulation of wind speed to wind power to capacity firming is demonstrated in the latter part of this paper using a Simulink-based DFIG wind farm model attached to the BESS-based MPC algorithm to show the performance of the proposed scheme. It uses real wind data measured at a local area in South Korea.

## 2. Problem Setup

This section describes the problem setup under consideration in this paper. Fig. 1 illustrates the integration of a wind farm with BESS using MPC. In general, the wind farm output is intermittent due to the stochastic nature of wind energy. In the proposed method, a BESS is employed in order to reduce the intermittency and improve the quality of the wind farm output by supplying the required or absorbing the excessed energy. In the course of charging and discharging the BESS, it is important for the proposed algorithm to make the system meet physical constraints on BESS, for example, the SoC (State-of-Charge) constraints.

Considering this, the objective of this paper is to make the output of the combined system of the wind farm and BESS track the given reference while satisfying the SoC constraints.

A first-order discrete-time model of the system is given by

$$E_b(k+1) = E_b(k) - t_d u(k) \tag{1}$$

$$y(k) = u(k) + P_w(k) \tag{2}$$

where $k$ denotes the sampling time, $E_b(k)$ denotes the stored energy or state-of-charge in the BESS, and $u(k)$ denotes the BESS charging/discharging power as the control input to the system. $P_w(k)$ is the generated power from the wind farm and $y(k)$ is the firmed output of the combined BESS + Wind Farm. The $t_d$ is the power conversion coefficient (MW to MWh). Considering the physical limitations of the BESS, the state $E_b(k)$ and $u(k)$ should satisfy the constraints

$$u_{\min} \le u(k) \le u_{\max}, \quad \forall k, \tag{3}$$

$$E_{\min} \le E_b(k) \le E_{\max}, \quad \forall k. \tag{4}$$

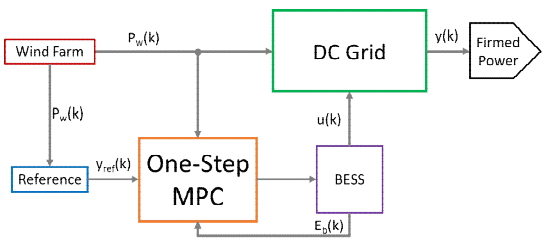


**Fig. 1.** System block diagram

Constraint (3) denotes the limitation on the power output of the BESS and inequality (4) implies the SoC constraint. It is assumed that $u_{min}$ is negative.

In terms of the mathematical model, the objective is to devise a charging and discharging strategy $u(k)$ such that it drives the output $y(k)$ to the desired reference $y_{ref}(k)$ with fulfilling the constraints.

## 3. Main Result

This section presents two optimal charging and discharging strategies for capacity firming.

### 3.1 One-step MPC based strategy

The proposed charging and discharging strategy is obtained by solving the following optimization problem at every sampling instant

$$\min_{u(k)} J(u(k)) \tag{5}$$

subject to (3) and (4)

where

$$J(u(k)) = \alpha(y(k) - y_{ref}(k))^2 + \beta(u(k))^2 \tag{6}$$

and $\alpha$ and $\beta$ are tuning parameters.

Using this optimization problem with the cost function, the optimal $u(k)$ makes output $y(k)$ converge to $y_{ref}(k)$ using minimal energy over the prediction horizon.

Note that, without considering the constraints in (3) and (4), the unconstrained optimal input $u_{uc1}(k)$ of (6) is given by

$$u_{uc1}(k) = -\frac{\alpha\left(P_w(k) - y_{ref}(k)\right)}{(\alpha+\beta)}. \tag{7}$$

**Theorem 1:** The optimal control $u^*(k)$ of optimization problem (5) is given by

$$u^*(k) = \begin{cases} u_a, & if\ u_{uc1}(k) > u_a \\ u_{uc1}(k), & otherwise \\ u_b, & if\ u_{uc1}(k) < u_b \end{cases} \tag{8}$$

where

$$u_a = \min\left\{u_{\max}, \frac{E_b(k) - E_{\min}}{t_d}\right\},$$

$$u_b = \max\left\{u_{\min}, \frac{E_b(k) - E_{\max}}{t_d}\right\}.$$

***Proof***: If $E_b(k)$ meets constraint (4), $u(k)$ needs to be determined such that $E_b(k+1)$ also satisfies the constraint.

In view of Equation (1), if $u(k)$ is determined so as to satisfy

$$E_{\min} \le E_b(k) - t_d u(k) \le E_{\max} \tag{9}$$

then, $E_b(k+1)$ satisfies the constraint, i.e.

$$E_{\min} \le E_b(k+1) \le E_{\max}.$$

Inequality (9) can be written as

$$\frac{E_b(k) - E_{\max}}{t_d} \le u(k) \le \frac{E_b(k) - E_{\min}}{t_d}.$$

Hence, the two constraints (3) and (4) are satisfied if the control input $u(k)$ satisfies the following inequality

$$u_b \le u(k) \le u_a. \tag{10}$$

Since the cost function $J$ is nothing but a quadratic function in $u(k)$, the optimal control $u^*(k)$ is given by (8) considering the unconstrained optimal solution (7) and the constraint (10). ■

In such an optimization based decision making, it is quite important to guarantee recursive feasibility. In other words, if the optimization problem is initially feasible, it has to be always feasible thereafter. In the case of optimization problem (5), since $u(k)=0$ is always a feasible input, the problem is always feasible. Since the problem always has a feasible solution, $E_b(k)$ is bounded for all time instant in light of constraint (4).

### 3.2 One-step MPC strategy with SoC tracking

Since BESS is quite an expensive equipment, it is quite important to use it in a way that its lifetime becomes prolonged as possible. To this end, it is crucial to maintain SoC such that it stays in a prespecified intervals or close a desired level.

Taking this observation into account, consider the following optimization

$$\min_{u(k)} J_m(u(k)) \quad \text{subject to (3) and (4)} \tag{11}$$

where

$$\begin{aligned} J_m(u(k)) = {} & \alpha(y(k) - y_{ref}(k))^2 \\ & + \gamma(E_b(k+1) - E_{ref})^2 + \beta(u(k))^2, \end{aligned} \tag{12}$$

$\gamma$ and $E_{ref}$ are tuning parameters, and $E_{ref}$ implies the desired SoC level.

This second optimization problem utilizes a cost function which is similar to cost function (6), but with an additional term which aims to maintain the SoC to a desired level.

In this case, the unconstrained optimal input $u_{uc2}(k)$ of (11) is given by

$$u_{uc2}(k) = -\frac{\alpha\left(P_w(k) - y_{ref}(k)\right)}{(\alpha + \beta + \gamma t_d^{\,2})} - \frac{\gamma t_d \left(E_{ref} - E_b(k)\right)}{(\alpha + \beta + \gamma t_d^{\,2})}. \tag{13}$$

The resulting optimal solution is given by

$$u^*(k) = \begin{cases} u_a, & \text{if } u_{uc2}(k) > u_a \\ u_{uc2}(k), & \text{otherwise} \\ u_b, & \text{if } u_{uc2}(k) < u_b \end{cases} \tag{14}$$

The derivation is quite similar to the previous case.

In the next section, the simulation results of both cost functions $J$ and $J_m$ are presented.

## 4. Simulation

For the simulation, two different setups were made. Each setup is simulated using the cost functions $J$ and $J_m$.

Section 4.1 shows a charging-discharging simulation using the proposed scheme in which real measured wind power $P_w$ is used for the MPC scheme to generate the firmed wind power. Section 4.2 demonstrates a Simulink-based, real-time, charging-discharging simulation results in which real measured wind speed data $V_w$ is injected into a wind farm library to generate power $P_w$ and this generated power $P_w$ simultaneously is combined with BESS equipped with the proposed MPC scheme to generate the firmed wind power.

All simulations are done in MATLAB 2016a [11].

### 4.1 Simulation setup using measured wind power $P_w$

For the first simulation, the input $P_w$ is taken from a real wind power data from a 28 MW windfarm in Gochang, North Jeolla in South Korea. The data was measured in January of 2014. From that raw data, the wind power $P_w$ is constructed by taking a portion of the data series and resampling it so that each new interval is just the average of the original data series.

The $y_{ref}$ is the smoothing reference, and for this simulation, this reference is constructed from the data of $P_w$ by taking its mean for a given dispatch interval. The dispatch interval was predetermined (e.g. 1 dispatch period = 6 sampling time), so that the smoothing reference $y_{ref}$ changes after every 6th sampling time.

The constraints of the BESS are defined by the energy capacity $E_{max}$ and power capacity $u_{max}$. For this simulation, we set $E_{max}$ to 4 MWh and $u_{max}$ to 4 MW. The lower limit $E_{min}$ is set to 0 MWh and $u_{min}$ to -4 MW.

Given this setup, the simulation is executed using the

two cost functions defined in (5) and (11). The results are shown in Sections 4.1.1 and 4.1.2.

### *4.1.1 Wind firming simulation result using cost function J*

Figs. 3-5 show the results of the MPC scheme using the optimal solution (8) derived from the cost function in (5).

Fig. 3 shows the comparison between the original wind power input ($P_w$) versus the firmed power output of the combined BESS and windfarm ($y$). The smoothing reference ($y_{ref}$) is also shown on the graph.

Figs. 4 and 5 show the graphs of $u(k)$ and $E_b(k)$. Fig. 4 shows the control input power $u(k)$ of the BESS. The positive value indicates a discharging state from the BESS while the negative value indicates a charging state. Fig. 5 shows the energy stored inside the BESS, which is synonymous to the state-of-charge of the battery. By observing Fig. 4, we can see that the BESS has more charging (negative) phases than discharging phases (positive), and this translates to an overall increase in the battery's energy as shown in Fig. 5.

The result in Fig. 3 shows how the firmed power (Fig. 3, black) approaches the reference line (Fig. 3, blue) effectively, making the firming successful. It should also be observed that the input $u(k)$ always satisfy the constraints as seen in Fig. 4. Both the input $u$ and the state $E_b$ were adequately bounded, thus, firming is successfully achieved with constraints satisfaction.

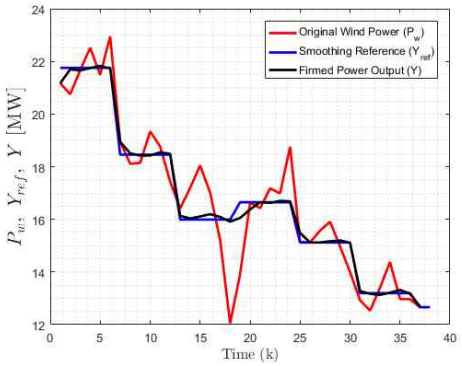


**Fig. 3.** Original wind power vs firmed power output (cost function $J$)

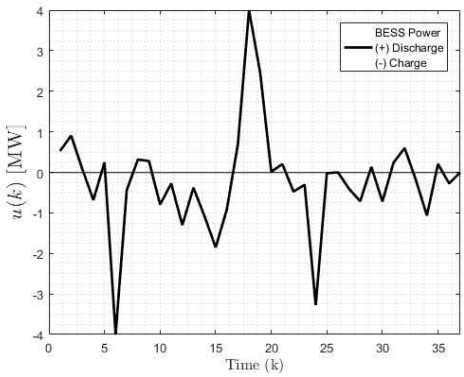


**Fig. 4.** BESS power ($-4 \le u(k) \le 4, \forall k$ )

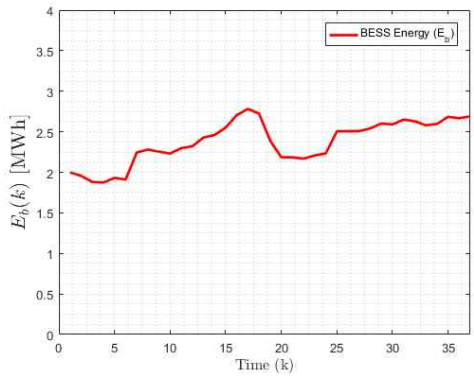


**Fig. 5.** BESS energy ($0 \le E_b(k) \le 4, \forall k$ )

### *4.1.2 Wind firming simulation result using cost function $J_m$*

This section employs the same setup defined in 4.1 but uses the optimal solution (14) derived from the secondary cost function in (11), with an addition of a secondary reference $E_{ref}$. This additional $E_{ref}$ is the reference for the energy of the BESS. For this simulation, we set $E_{ref}$ to a constant value of 2, which depicts 50% energy charge.

Fig. 6 shows the similar graph with Fig. 3, comparing

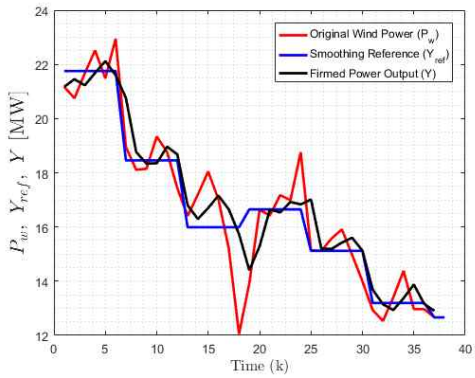


**Fig. 6.** Original wind power vs firmed power output (cost function $J_m$)

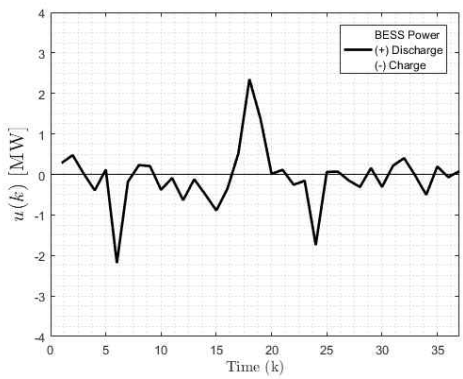


**Fig. 7.** BESS power ($-4 \le u(k) \le 4, \forall k$ ) (COST function $J_m$)

the original wind power input ($P_w$) versus the firmed power output ($y$) along with the smoothing reference ($y_{ref}$).

Figs. 7 and 8 show the graphs of $u(k)$ and $E_b(k)$. These two graphs are similar to Figs. 4 and 5 in the first case.

For this simulation, the cost function $J_m$ puts emphasis on keeping the BESS energy $E_b$ close to $E_{ref}$ as much as possible. Fig. 8 shows the improved SoC behavior due to this modified cost equation. Fig. 6 shows that the firmed power output $y$ still tracks the smoothing reference $y_{ref}$, although not as good as the previous result in Fig. 3. This is because the cost function was configured to put more emphasis on tracking $E_{ref}$ over $y_{ref}$. This compromise between the two references makes tuning of the cost function delicate. By proper tuning, a good balance between the output firming and improved SoC behavior can be achieved.

### 4.2 Real-time simulink-based simulation using wind farm DFIG model [11] with wind speed $V_w$ as input

For realistic simulation, a second simulation setup is made using Simulink where we used a wind speed profile as input and converted it to wind power before sending it to our capacity firming scheme. The conversion of wind energy to wind power is made possible by using a pre-made Wind Farm DFIG Phasor model [11] which is included in MATLAB 2016a. Fig. 9 shows the overview of the whole Simulink setup.

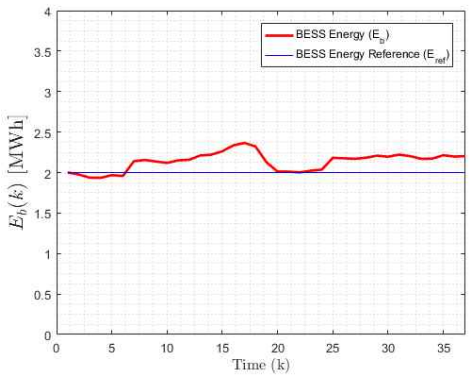


**Fig. 8.** BESS energy ($0 \le E_b(k) \le 4, \forall k$ ) (cost function $J_m$)

Fig. 9 contains the following: a 9-MW DFIG wind farm (right rectangle) connected to a 25-kV distribution system exports power to a 120-kV grid through a 30-km, 25-kV feeder (left rectangle). The proposed BESS MPC scheme is added on the bottom left circle. For the simulation, the input of the DFIG wind turbine was modified such that it can accept a wind speed data array $V_w$. The wind speed data is made out of one-hour average interval, and it was taken from a real wind profile measured in Jeju, South Korea during January of 2014. During simulation, the 9-MW DFIG wind turbine generates electrical power from this wind speed profile in real-time, and this power output is discretized into $P_w$ so that it can be used as input to our Simulink version of the proposed scheme (encircled block).

Fig. 10 shows the inside schematic of the BESS MPC block. The left part shows two inputs: the first one is the smoothing reference $y_{ref}$, while the second one is the wind power $P_w$. For this simulation, the smoothing reference $y_{ref}$ are derived from $P_w$ itself, and is generated by using the forecasting technique called Persistence method [1]. The Persistence method is a forecasting technique where the current value of the $P_w(k)$ is used as a reference for the future time steps depending on how long is the forecast horizon (e.g. $[P_w(k+1) \ \ldots \ P_w(k+N)] = P_w(k)$). For this simulation, the current value of $P_w(k)$ is held for the whole dispatch interval of the next step. One dispatch interval is 60 seconds. Since the output of the DFIG turbine is continuous, both the $y_{ref}$ and $P_w$ signal are discretized using zero-order hold to match the discrete time setting of the MPC scheme. The state-of-charge $E_b$, which is represented in Fig. 10 as state $x$, is driven back to the MPC controller to complete the feedback loop of the system. The signals $P_w$, $y$, and $y_{ref}$ are combined in one graph to show the

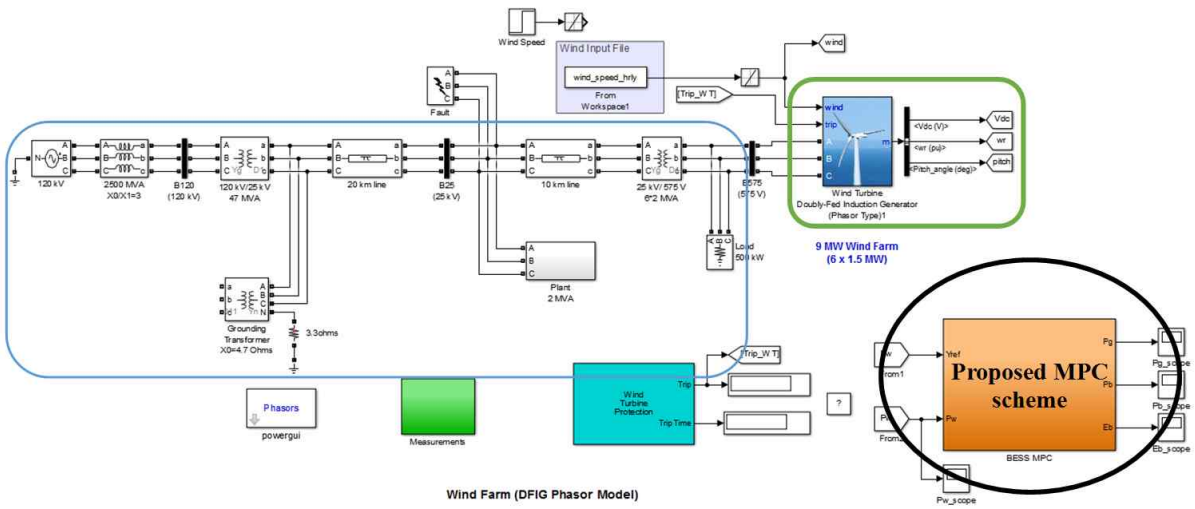


**Fig. 9.** Simulink's wind farm DFIG phasor model [11] with BESS MPC control

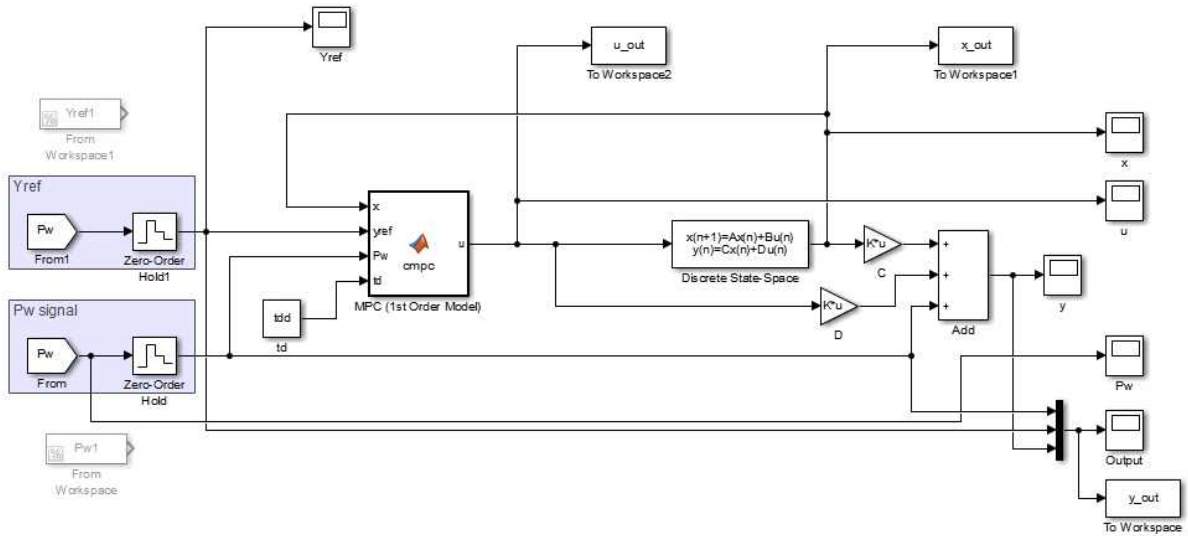


**Fig. 10.** Internal schematic of the proposed BESS-MPC scheme

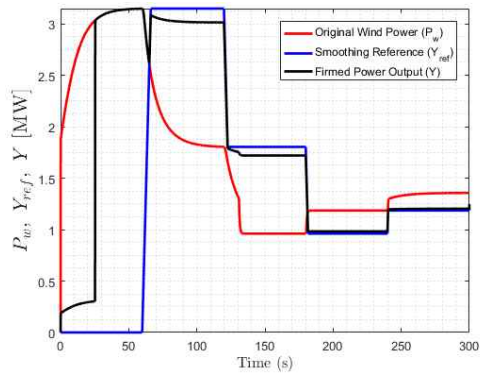


**Fig. 11.** Original wind power vs firmed power output (cost function $J$)

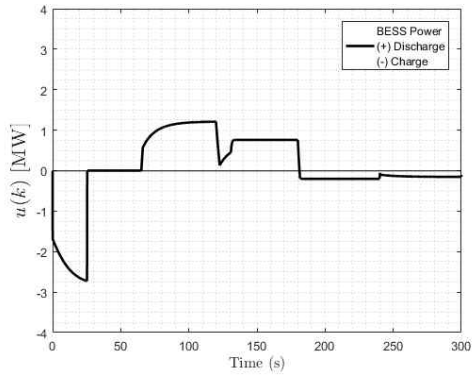


**Fig. 12.** BESS power ($-4 \le u(k) \le 4, \quad \forall k$ ) (cost function $J$)

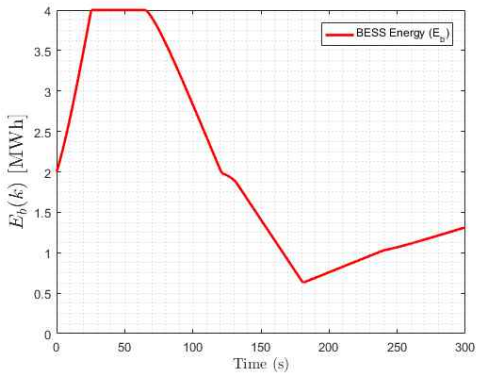


**Fig. 13.** BESS Energy ($0 \le E_b(k) \le 4, \quad \forall k$ ) (cost function $J$)

comparison of the input vs output vs reference.

The physical constraints of the BESS are again defined. For the power rating (Fig. 12), $u_{max}$= 4 MW, $u_{min}$= -4 MW. For the energy capacity (Fig. 13), $E_{max}$ = 4 MWh, $E_{min}$ = 0.

Given this Simulink setup, two simulations of the MPC schemes are done using the cost functions defined in (5) and (11) as proposed in Section 3. The results of these two simulations are shown in Sections 4.2.1 and 4.2.2.

### *4.2.1 Real-time simulink-based wind firming simulation result using cost function J*

This section shows the result of the Simulink-based MPC scheme using the optimal solution (8) derived from the cost function in (5).

Fig. 11 shows the comparison between the original wind power ($P_w$) versus the firmed power output of the combined BESS and windfarm ($y$). The smoothing reference ($y_{ref}$) is also displayed on the graph.

Figs. 12 and 13 show the graphs of $u(k)$ and $E_b(k)$. Fig. 12 is the graph of the power charged/discharged by the BESS which is controlled by the MPC scheme. Fig. 13 shows the energy stored inside the BESS, which also depicts the state-of-charge of the battery.

Fig. 11 shows that the firmed power (Fig. 11, black) follows the reference line (Fig. 11, blue) effectively, except for the part where the energy of the BESS is fully charged (around 30-60 secs). During this time, the firmed output (Fig. 11, black) behaves the same way as the original wind power (Fig. 11, red) since the firmed power receives 0

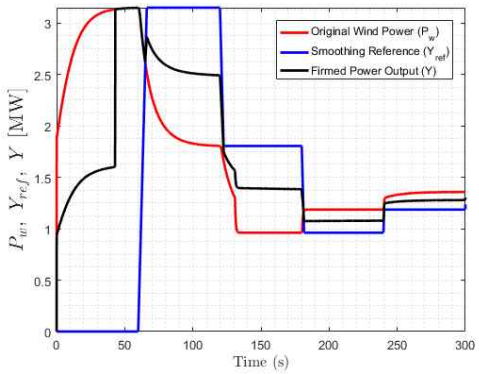


**Fig. 14.** Original wind power vs firmed power output (cost function $J_m$)

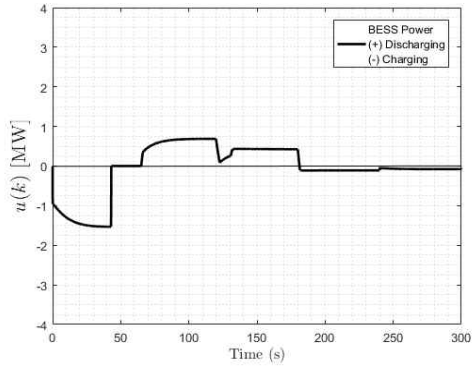


**Fig. 15.** BESS power ($-4 \leq u(k) \leq 4, \forall k$ ) (cost function $J_m$)

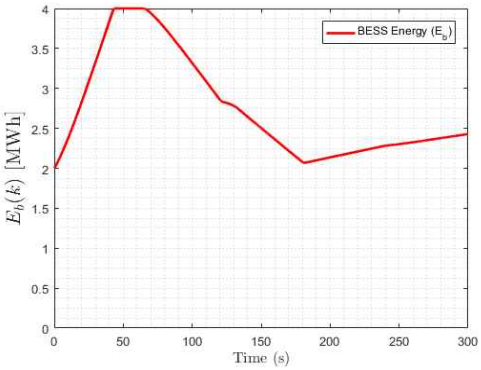


**Fig. 16.** BESS energy ($0 \leq E_b(k) \leq 4, \forall k$ ) (cost function $J_m$)

input from $u(k)$ as seen in Fig. 12 (30-60 secs). The fully charged status of the BESS can be seen in Fig. 13 around the same time duration. While the MPC algorithm can successfully satisfy the constraints whenever they are reached, tracking performance, on the other hand, is lost whenever these boundaries are reached. This problem can be avoided by setting a larger constraint, but in the real world, increasing the limits of BESS may not be an option. Using better forecasting of the wind and considering the economics of the power generation can improve the firming behavior by generating a better reference that will maximize the BESS capacity or maximize profit.

#### *4.2.2 Real-time simulink-based wind firming simulation result using cost function $J_m$*

The last simulation applies the Simulink-based MPC scheme using the optimal solution (14) derived from the cost function in (11).

Fig. 14 shows the similar comparison graph portrayed in Fig. 11. Comparing these two figures, it can be observed how the firmed result in Fig. 14 is farther from the smoothing reference than the result in Fig. 11. This is because our second cost function puts more weight on tracking $E_{ref}$ than $y_{ref}$. The tuning of relative weight for these two references is done in the cost function defined in (12).

Figs. 15 and 16 show the graphs $u(k)$ and $E_b(k)$. Comparing Fig. 12 from the previous simulation with Fig. 15 shows less power supplied compared to Fig. 12. However, this also translates into a better SoC performance, as shown in Fig. 16, where the variation of energy charge is kept to a minimum compared to Fig. 13, due to the existence of $E_b$ tracking $E_{ref}$ in the cost function. The value of $E_{ref}$ is set to 2, which is the same value with the simulation in Section 4.1.2.

The second cost function $J_m$ gives an improved SoC performance, but at the expense of losing tracking of the firmed output y to a certain extent. Proper tuning of the second cost function can provide a good balance between reliable power firming and taking good care of the BESS's lifetime.

## 5. Conclusion

This paper proposed two 1-step MPC strategies for wind farm capacity firming using BESS. The first strategy employs optimization to generate the required BESS power to firm the wind power output to the desired reference level without violating any physical constraints. The second strategy uses an alternative cost function that also firms the wind power output, but at the same time regulate the variation of the BESS energy to a minimum without violating any physical constraints. Simulation results using wind farm library in Simulink and real measured wind data show that the proposed scheme results in not only successful capacity firming but also satisfaction of physical constraints in BESS.

## Acknowledgements

This research was supported by Basic Science Research Program through the National Research Foundation of Korea (NRF) funded by the Ministry of Education (NRF-2015R1D1A1A01060588) and by the Human Resources Development of the Korea Institute of Energy Technology Evaluation and Planning (KETEP) grant funded by the Korea government Ministry of Trade, Industry & Energy (20154030200720).

## References


[1] S. S. Soman, H. Zareipour, O. Malik, and P. Mandal, "A review of wind power and wind speed forecasting methods with different time horizons," in *North American Power Symposium* (*NAPS*), pp. 1-8, 2010.

[2] M. Lei, L. Shiyan, J. Chuanwen, L. Hongling, and Z. Yan, "A review on the forecasting of wind speed and generated power," *Renew. Sustain. Energy Rev.*, vol. 13, no. 4, pp. 915-920, May 2009.

[3] J. K. Lyu, J. H. Heo, M. K. Kim, and J. K. Park, "Impacts of Wind Power Integration on Generation Dispatch in Power Systems," *Journal of Electrical Engineering and Technology*, vol. 8, no. 3, pp. 453-463, 2013.

[4] A. M. Howlader, N. Urasaki, A. Yona, T. Senjyu, and A. Y. Saber, "A review of output power smoothing methods for wind energy conversion systems," *Renew. Sustain. Energy Rev.*, vol. 26, pp. 135-146, Oct. 2013.

[5] S. Abdelrazek and S. Kamalasadan, "Integrated control of battery energy storage management system considering PV capacity firming and energy time shift applications," in *2014 IEEE Industry Application Society Annual Meeting*, pp. 1-7, 2014.

[6] Z. Wei, B. Y. Moon, and Y. H. Joo, "Smooth Wind Power Fluctuation Based on Battery Energy Storage System for Wind Farm," *Journal of Electrical Engineering and Technology*, vol. 9, no. 6, pp. 2134-2141, 2014.

[7] C. L. Nguyen, H. H. Lee, and T. W. Chun, "Cost-Optimized Battery Capacity and Short-Term Power Dispatch Control for Wind Farm," *IEEE Trans. Ind. Appl.*, vol. 51, no. 1, pp. 595-606, Jan. 2015.

[8] C. L. Nguyen and H. H. Lee, "Effective power dispatch capability decision method for a wind-battery hybrid power system," *Transm. Distrib. IET Gener.*, vol. 10, no. 3, pp. 661-668, 2016.

[9] T. K. A. Brekken, A. Yokochi, A. von Jouanne, Z. Z. Yen, H. M. Hapke, and D. A. Halamay, "Optimal Energy Storage Sizing and Control for Wind Power Applications," *IEEE Trans. Sustain. Energy*, vol. 2, no. 1, pp. 69-77, Jan. 2011.

[10] A. Khatamianfar, "Advanced Discrete-Time Control Methods for Industrial Applications," *ArXiv150404423 Cs*, Ph.D. dissertation, School of Electrical Eng. and Telecommunications, UNSW, Sydney, Australia, pp. 18-68, Apr. 2015.

[11] MATLAB and Simscape Power Systems 2016a, "Wind Farm DFIG Phasor Model (power_wind_dfig)," The MathWorks, Inc., Natick, Massachusetts, United States, 2016.


**Micro Daryl Robles** received his B.S. degree in Electronics and Communications Engineering from University of the Philippines, Diliman in 2012. He is currently an M.S. student at Seoul National University of Science and Technology, Korea. His research interests include optimal control using model predictive control, power system frequency regulation, wind power firming and microgrid.

**Jung-Su Kim** He received BS., MS., and Ph.D degree in electrical engineering from Korea University. Since 2009 he has been with Dept. of Electrical and Information Engineering, Seoul Nat'l University of Science and Technology. His research interest includes MPC and its application to energy systems.

**Hwachang Song** received B.S., M.S., and Ph.D. degrees in Electrical Engineering from Korea University in 1997, 1999, and 2003, respectively. He was a Post-Doctoral Visiting Scholar at Iowa State University, U.S., from 2003 to 2004. He was a Faculty Member with the School of Electronic and Information Engineering, Kunsan National University, Korea, from 2005 to 2008. Currently, he is an Associate Professor with the Department of Electrical and Information Engineering, Seoul National University of Science & Technology, Korea. His research interests include nonlinear optimization, power system stability and control, battery energy storage systems, and system modeling.